Preprint
UCRL-JC-151293

Intergrowth Structure in U- and Hf-Bearing Pyrochlore and Zirconolite: TEM Investigation

H. Xu, Y. Wang, P. Zhao, W. L. Bourcier, R. Van Konynenburg, and H. F. Shaw

This article was submitted to 2002 Materials Research Society Fall Meeting, Boston, Massachusetts, Dec. 2-6, 2002

December 4, 2002

U.S. Department of Energy
Lawrence Livermore National Laboratory

Intergrowth structure in U- and Hf-bearing pyrochlore and zirconolite: TEM investigation

Huifang Xu[1], Yifeng Wang[1, 2], Pihong Zhao[3], William L. Bourcier[3], Richard Van Konynenburg[3], and Henry F. Shaw[3]

1. Transmission Electron Microscopy Laboratory, Department of Earth and Planetary Sciences, The University of New Mexico, Albuquerque, New Mexico 87131, USA.
2. Sandia National Laboratories, Carlsbad, NM 88220, USA
3. Lawrence Livermore National Laboratory, L-219, Livermore, CA 94550, USA
E-mail: hfxu@unm.edu

Abstract

Transmission electron microscopy results from a sintered ceramics with stoichiometry of $Ca(U_{0.5}Ce_{0.25}Hf_{0.25})Ti_2O_7$ show the material contains both pyrochlore and zirconolite phases and structural intergrowth of zirconolite lamellae within pyrochlore. (001) plane of zirconolite is parallel to (111) plane of pyrochlore because of their structural similarities. The pyrochlore is relatively rich in U, Ce, and Ca with respect to the coexisting zirconolite. Average compositions for the coexisting pyrochlore and zirconoliteproduced by sintering at 1350 °C are $(Ca_{1.01}Ce^{3+}_{0.13}Ce^{4+}_{0.19}U_{0.52}Hf_{0.18})(Ti_{1.95}Hf_{0.05})O_7$ (with U/(U+Hf) (in the AB sites) = 0.74) and $(Ca_{0.91}Ce_{0.09})(Ce^{3+}_{0.08}U_{0.26}Hf_{0.66}Ti_{0.01})Ti_{2.00}O_7$ (with U/(U+Hf) = 0.28) respectively. A single pyrochlore ($(Ca,U,Hf)_2Ti_2O_7$) phase may be synthesized at 1350 °C if the ratio of U/(U+Hf) is greater than 0.72, and a single zirconolite ($Ca(Hf,U)Ti_2O_7$) phase may be synthesized at 1350 °C if the ratio of U/(U+Hf) is less than 0.28. An amorphous leached layer that is rich in Ti and Hf forms on the surface after the ceramics has been leached in pH 4 buffered solution. The thickness of the layer ranges from 5 nm to 15 nm. It is suggested that under these conditions, the leached layer functions as a protective layer, and reduces the leaching rate over time.

1. Introduction

A durable titanate ceramic waste form similar to Synroc [2] containing pyrochlore ($Ca(U,Pu)Ti_2O_7$) and zirconolite ($CaZrTi_2O_7$), a derivative structure of pyrochlore, as major crystalline phases has been shown to be particularly promising for immobilizing wastes containing fissile elements (^{239}Pu and ^{235}U) [1-12]. The general stoichiometry of zirconolite and pyrochlore can be expressed as $ABTi_2O_7$. In the monoclinic zirconolite structure, the A and B sites are distinct, while in the cubic pyrochlore structure, they are equivalent. Tetravalent actinides generally occupy site B positions with coordination number of 7 or 8. Thermodynamic study indicates that U- and Pu-pyrochlore phases are stable with respect to rutile, perovskite, and the oxides UO_2 and PuO_2 [12]. However, Th-pyrochlore is unstable with respect to rutile, perovskite, and ThO_2 [12]. The ceramic waste form will be thermodynamically stable in aqueous silica-depleted and aqueous carbonate-depleted groundwater environments (such as the WIPP site in salt) [13].

The concept of Synroc was originally proposed by Ringwood et. al. [2] and the first Synroc fabrication technology was developed by Dosch et al. [1]. During the last two decades, Synroc and related ceramic wasteforms have been subjected to extensive studies [1-14]. These wasteforms immobilize radionuclides by incorporating them into appropriate solid-solution phases. Because they contain phases with large coordination polyhedra, (with coordination numbers ranging from 7 to 8) in their structures, ceramics are able to accommodate a wide

range of radionuclides (e.g., actinides, Pu, U, Ba, Sr, Cs, Rb, Tc, etc.) as well as neutron absorbers (e.g., Gd and Hf) [10]. U- and Pu-loaded ceramic generally contains pyrochlore and zirconolite [1, 2, 3, 7, 8, 15]. Various Synroc formulations (e.g., Synroc-C, Synroc-D, Synroc-E, Synroc-F etc.) have been developed for specific high level wastes [1, 15, 16]. Homogeneity of sintered ceramics is an important factor to long-term chemical durability.

2. Samples and experiments

The starting material with stoichiometry of $Ca(U_{0.5}Ce_{0.25}Hf_{0.25})Ti_2O_7$ was prepared by mixing and grinding powders of TiO_2 (anatase), UO_2, $Ca(OH)_2$, and CeO_2 with deionized water. Ce was used as a nonradioactive analog for Pu in the ceramics studied here. The mixed material was dried overnight in air at about 90 °C. The dried material was pressed and then sintered at 1350°C for 5 hours in an environment of slowly flowing Ar gas at one atmosphere. Part of the sintered sample was crushed in acetone. Drops of acetone suspension containing the crushed particles were dropped on holey C-coated nylon grids for transmission electron microscopy (TEM) observation. Dissolution tests were carried out by using single-pass flow-through methods [24]. All TEM and energy-dispersive spectroscopy (EDS) results were carried out with a JEOL 2010F FEG-TEM and associate Gatan GIF system, and a 2010 high-resolution TEM and Oxford Link ISIS EDS system. Point-to-point resolution of the high-resolution TEM is 0.19 nm. Mineral standards were used for quantification of collected EDS data as that described in reference [17]. We used a theoretical k_{Ce} value, because no Ce-silicate standard was available for Ce. Electron energy-loss spectroscopy (EELS) studies of Ce were carried out with a JEOL 2010F HRTEM equipped with a GIF system.

3. Results and discussions

TEM and EDS results show that the sample contains both pyrochlore and zirconolite phases in a relative abundance ratio of 10:1. Figure 1 shows a selected-area electron diffraction (SAED) pattern and high-resolution TEM image of the pyrochlore. EDS spectra show that the pyrochlore is relatively rich in U, Ce, and Ca with respect to the coexisting zirconolite (Figure 2). EELS data indicate that Ce in zirconolite is in the form of Ce^{3+}, and Ce in the pyrochlore is present as both Ce^{3+} and Ce^{4+}, with $Ce^{4+}/(Ce^{4+} + Ce^{3+}) \sim 0.6$, as determined from the intensity ratio of the M4 and M5 edges [18, 19] (Figure 2). Ce^{4+} is sensitive to high-energy electron beam. A defocused beam was used for collecting the EELS spectra to avoid reduction of Ce^{4+}. The composition of the pyrochlore and zirconolite as determined from EDS spectra and EELS data are given in Table 1.

In some pyrochlore grains, there are zirconolite lamellae within pyrochlore. The (001) plane of zirconolite is parallel to the (111) of pyrochlore. A similar observation was also reported by Buck et al. [20]. The cell parameters measured from the SAED patterns are a = 10.5 Å for the pyrochlore (cubic) and a = 12.5 Å, b = 7.4 Å, c = 11.6 Å, β = 100° for zirconolite (monoclinic) respectively. A high-resolution TEM image shows the interface between pyrochlore and zirconlite is straight and coherent. The value of d_{111} (6.1 Å) of the pyrochlore is slightly larger than d_{002} (5.7 Å) of the zirconolite, because the pyrochlore contains more U (large ionic radius) than the zirconolite does (Table 1). The compositions of the zirconolite lamellae and the neighboring pyrochlore are also listed in Table1. Such lamella result from epitaxial growth during the crystallization of both pyrochlore and zirconolite. The (001) plane of zirconolite is very similar to the (111) plane of pyrochlore [21, 22]. In some areas, the zirconolite lamellae display a disordered structure that results from non-periodic stacking of 2-layer and 3-layer zirconolite polytypes as that occurs in Zr-zirconolite [17].

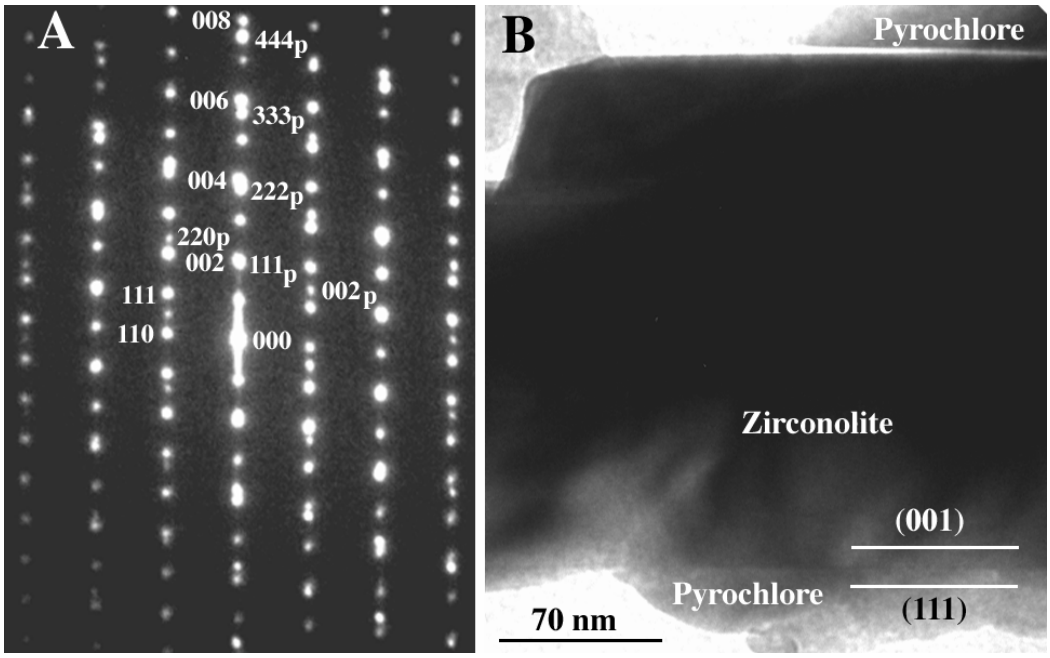

Figure 1 SAED pattern (A) and bright-field TEM image (B) from an area containing intergrown zirconolite and pyrochlore. (001) of zirconolite is parallel to (111) of pyrochlore.

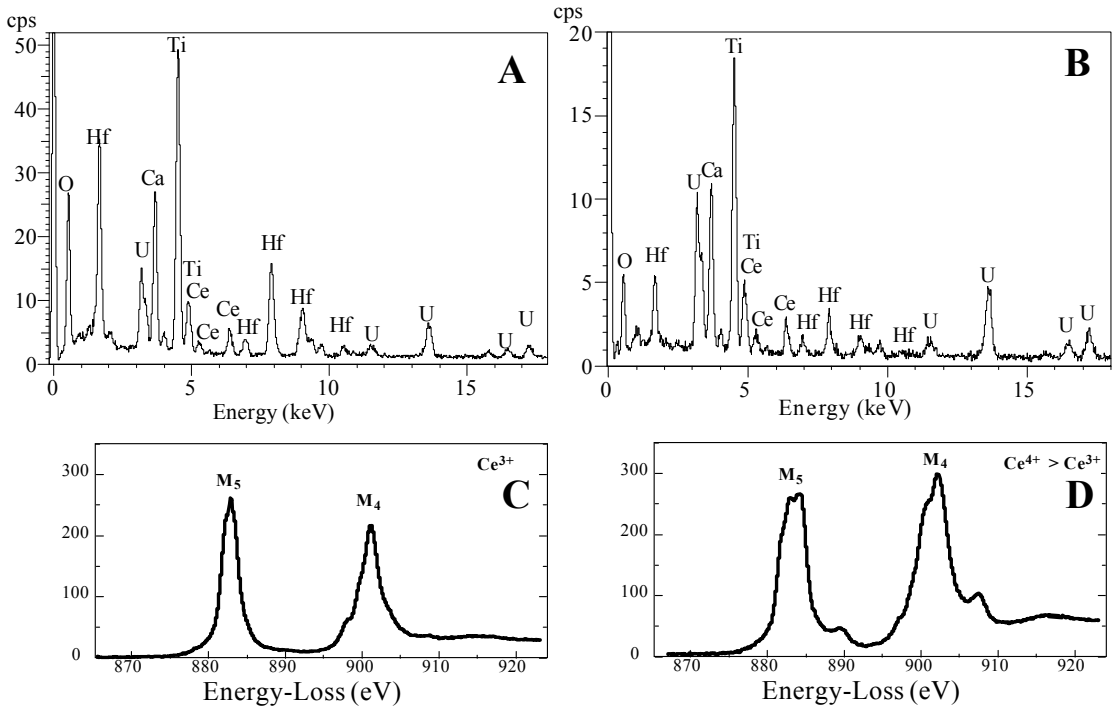

Figure 2 EDS spectra from zirconolite (A) and pyrochlore (B); EELS spectra from zirconolite (C) and pyrochlore (D).

Our EDS and TEM data indicate that there is a compositional gap between U-pyrochlore ($CaUTi_2O_7$) and Hf-zirconolite ($CaHfTi_2O_7$) at 1350 °C. The ratios of U/(U+Hf) in the B site of ABTI2O7 are 0.74 for pyrochlore and 0.28 for the zirconolite (in the case of pyrochlore, the "B site" is taken as meaning half of the equivalent AB sites) (Table 1). If all Hf atoms are at B site, then the ratio of U/(U+Hf) is 0.69 for the pyrochlore. Given the measured phase compositions, one calculates that there should be about 10 mole % zirconolite (including individual zirconolite grains and zirconolite lamellae within pyrochlore) in the mixture of pyrochlore and zirconolite with a bulk composition of $Ca(U_{0.5}Ce_{0.25}Hf_{0.25})Ti_2O_7$. This is in excellent agreement with the observed phase abundances in this sample. These data indicate that for the system studied here, a single phase pyrochlore ((Ca,U,Hf)Ti2O7) may be synthesized at 1350 °C if the ratio of U/(U+Hf) is larger than 0.74, and a single phase zirconolite ($Ca(Hf,U)Ti_2O_7$) may be synthesized at 1350 °C if the ratio of U/(U+Hf) is smaller than 0.28. Any mixtures with the U/(U+Hf) ratio between 0.74 and 0.28 will form a mixture of pyrochlore and zirconolite. The ionic radius difference between Pu^{4+} and Hf^{4+} is smaller than that between U^{4+} and Hf^{4+}. However, the chemical (Gibbs free energy of formation) difference between Pu^{4+} and Hf^{4+} is larger than that between U^{4+} and Hf^{4+} [23]. It can be inferred that the compositional gap between of $CaPuTi_2O_7$ and $CaHfTi_2O_7$ will be similar to that of $CaUTi_2O_7$ and $CaHfTi_2O_7$. The phase diagram may provide a guide for preparing single-phase ceramics for hosting U and Pu.

The single-pass flow-through experiments measured the release rates of elements dissolved from powdered ceramic into flowing pH-buffered solutions. They are designed to measure the dissolution rate far from equilibrium where rates are not affected by saturation effects. This is done by adjusting the flow rate and surface area of the sample. The release data are plotted as normalized release rate vs. time. (Fig. 3). The normalized release rate is defined as:

$$NR_i = \frac{(C_i^{out} - C_i^{in}) * q}{m * f_i * A}$$

where C_i^{in} is the concentration of element *i* in the blank buffered leach solution, C_i^{out} is the concentration of element *i* in the effluent solution, *q* is the solution flow rate, m is the mass of powdered ceramic used, f_i is the weight fraction of element *i* in the ceramic, and *A* is the BET-measured surface area of the ceramic. Normalized rates are given in units of g/(m^2 day). Also shown in the plot is the measured flow rate of buffered leach solution as a function of time.

A sample that was reacted at pH4 for 835 days at room temperature was selected for TEM investigation. TEM images show an amorphous layer on the grain surface. The thickness of the layer ranges from 5 nm to about 15 nm. Some of the thicker leached layers contain nanometer-sized TiO2 particles that appear to be crystallizing from the amorphous material. In general, the leached layer on pyrochlore is thicker than that on zirconolite, implying that the reaction rate of pyrochlore is faster than that of zirconolite. The results are consisting with the measurements from pure phases of zirconolite and pyrochlore [25]. EDS results from the leached samples indicate that the leached layer is rich in Ti and Hf, and poor in Ca and U. It is likely that the formation of such a stable layer will function as a protective layer and reduce the dissolution rate of the ceramics. The results also consist with the observation from naturally altered pyrochlore [19].

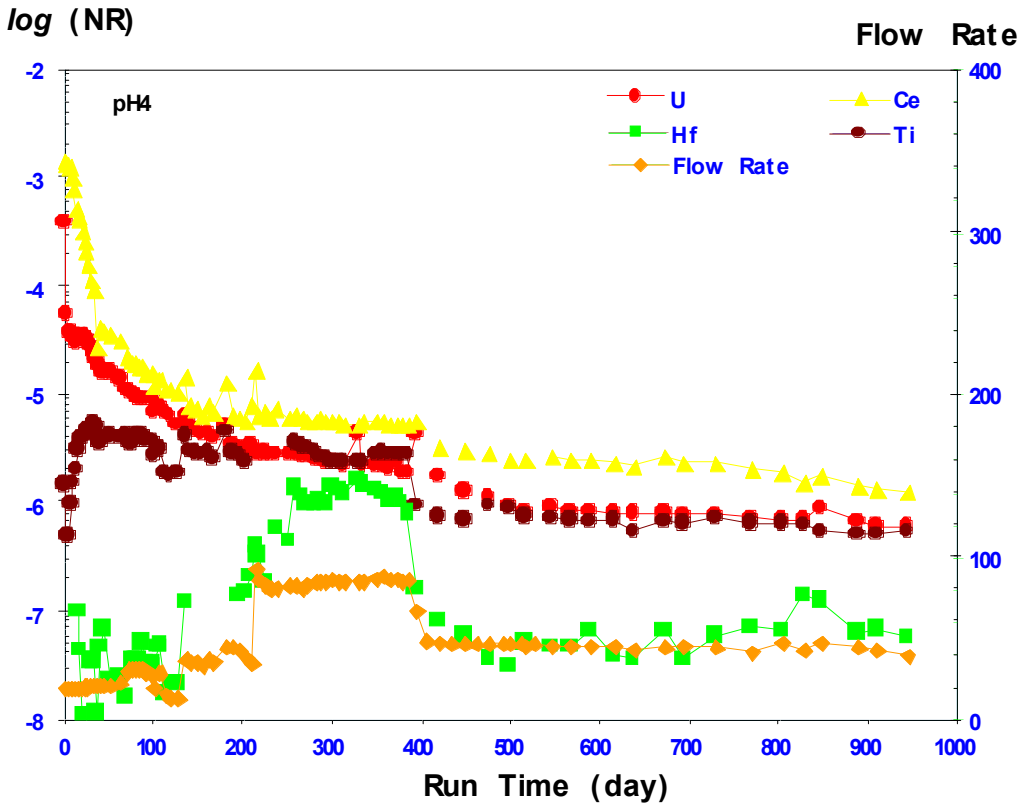

Figure 3 Normalized release rates (g/(m^2 day)) and flow rates (mL/day) of a Ce-surrogate pyrochlore-based ceramic formulation in pH 4 buffer solution.

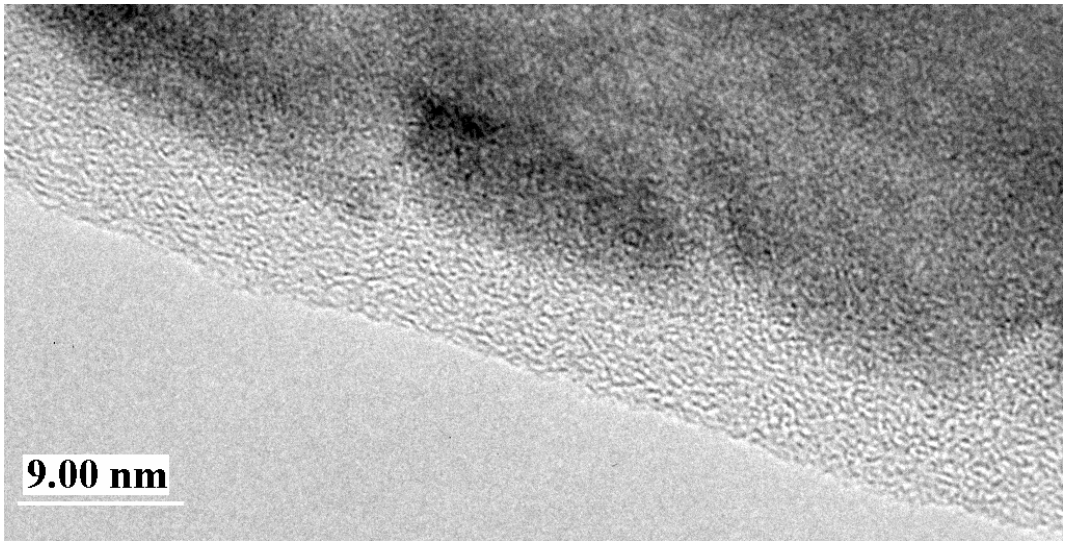

Figure 4 HRTEM image showing the leached amorphous layer that is rich in Ti and Hf. Lattice fringes in crystalline core are not so obvious because of the leached layer coating.

Table 1: Chemical formulae of the pyrochlore and zirconolite.

Pyrochlore	Zirconolite
$Ca_{0.99}(Ce^{3+}_{0.12}Ce^{4+}_{0.18}U_{0.52}Hf_{0.21})(Ti_{1.95}Hf_{0.05})O_7$	$(Ca_{0.91}Ce_{0.09})(Ce^{3+}_{0.10}U_{0.25}Hf_{0.66})(Ti_{1.99}Hf_{0.01})O_7$
$Ca_{1.02}(Ce^{3+}_{0.13}Ce^{4+}_{0.19}U_{0.54}Hf_{0.16})(Ti_{1.96}Hf_{0.04})O_7$*	$(Ca_{0.94}Ce_{0.06})(Ce^{3+}_{0.09}U_{0.25}Hf_{0.65}Ti_{0.01})Ti_{2.00}O_7$*
$Ca_{1.01}(Ce^{3+}_{0.13}Ce^{4+}_{0.19}U_{0.55}Hf_{0.15})(Ti_{1.95}Hf_{0.05})O_7$	$(Ca_{0.90}Ce_{0.10})(Ce^{3+}_{0.06}U_{0.25}Hf_{0.67})Ti_{2.00}O_7$
$Ca_{1.00}(Ce^{3+}_{0.13}Ce^{4+}_{0.18}U_{0.52}Hf_{0.19})(Ti_{1.96}Hf_{0.04})O_7$	$(Ca_{0.92}Ce_{0.08})(Ce^{3+}_{0.09}U_{0.26}Hf_{0.65})Ti_{2.00}O_7$
$Ca_{1.00}(Ce^{3+}_{0.13}Ce^{4+}_{0.19}U_{0.49}Hf_{0.21})(Ti_{1.94}Hf_{0.06})O_7$	$(Ca_{0.93}Ce_{0.07})(Ce^{3+}_{0.11}U_{0.26}Hf_{0.64})Ti_{2.00}O_7$
$Ca_{1.02}(Ce^{3+}_{0.12}Ce^{4+}_{0.18}U_{0.54}Hf_{0.18})(Ti_{1.94}Hf_{0.06})O_7$*	$(Ca_{0.88}Ce_{0.12})(Ce^{3+}_{0.05}U_{0.26}Hf_{0.66}Ti_{0.02})Ti_{2.00}O_7$*
	Average
$Ca_{1.01}(Ce^{3+}_{0.13}Ce^{4+}_{0.19}U_{0.52}Hf_{0.18})(Ti_{1.95}Hf_{0.05})O_7$	$(Ca_{0.91}Ce_{0.09})(Ce^{3+}_{0.08}U_{0.26}Hf_{0.66}Ti_{0.01})Ti_{2.00}O_7$
U/(U+ Hf) = 0.74	U/(U + Hf) = 0.26

Note: The chemical formulae are normalized to 7-oxygen. The formulae with * are from intergrown pyrochlore and zirconolite. The ratio of U/(U + Hf) only considers U and Hf in site B positions of zirconolite and pyrochlore with stoichiometry of $ABTi_2O_7$. The U/(U+ Hf) ratio for the pyrochlore is about 0.69 if all Hf atoms are on B sites.

Acknowledgment: This work is based upon research conducted at the Transmission Electron Microscopy Laboratory in the Department of Earth and Planetary Sciences of the University of New Mexico, which is partially supported by NSF (CTS98-71292), and State of New Mexico. This work was partially performed under the auspices of the U.S. Department of Energy by University of California Lawrence Livermore National Laboratory under contract No. W-7405-Eng-48.

REFERENCES

1. Dosch, R. G., Headley, T. J., Northrup, C. J., and Hlava, P. F., Sandia National Laboratories Report, Sandia 82-2980, 84pp (1982).
2. Ringwood, A. E., Kesson, S. E., Reeve, K. D., Levins, D. M., and Ramm, E. J., Synroc. In W. Lutze and R. C. Ewing eds., "Radioactive Waste Forms for the Future." North-Holland, Amsterdam, pp. 233-334 (1988).
3. Jostsons, A., Vance, E. R., Mercer, D. J., Oversby, V. M., In T. Murakami and R. C. Ewing eds. "Scientific Basis for Nuclear Waste Management XVIII." Materials Research Society, Pittsburgh, pp. 775-781 (1995).
4. Weber, W. J., Ewing, R. C., and Lutze, W., In W. M. Murphy and D. A. Knecht eds., "Scientific Basis for Nuclear Waste Management XIX." Materials Research Society, Pittsburgh, 25-32 (1996).
5. Bakel, A. J., Buck, E. C., and Ebbinghaus, B., (1997) In "Plutonium Future — The Science." Los Alamos National Laboratories, 135-136 (1997).

6. Begg, B. D., and Vance, E. R., In W. J. Gray and I. R. Triay eds. “Scientific Basis for Nuclear Waste Management XX.” Materials Research Society, Pittsburgh, 333-340 (1997).
7. Begg, B. D., Vance, E. R., Day, R. A., Hambley, M., and Conradson, S. D. In W. J. Gray and I. R. Triay eds. “Scientific Basis for Nuclear Waste Management XX.” Materials Research Society, Pittsburgh, 325-332 (1997).
8. Buck, E. C., Ebbinghaus B., Bakel, A. J., and Bates, J. K., (1997) Characterization of a plutonium-bearing zirconolite-rich Synroc. In W. J. Gray and I. R. Triay eds. “Scientific Basis for Nuclear Waste Management XX.” Materials Research Society, Pittsburgh, 1259-1266.
9. Vance, E. R., MRS Bulletin, vol. XIX, p. 28-32 (1994).
10. Vance, E. R., Jostsons, A., Stewart, M. W. A., Day, R. A., Begg, B. D., Hambley, M. J., Hart, K. P., and Ebbinghaus, B. B., In "Plutonium Future — The Science." Los Alamos National Laboratories, 19-20 (1997a).
11. Vance, E. R., Hart, K. P., Day, R. A., Carter, M. L., Hambley, M., Blackford, M. G., and Begg, B. D., In W. J. Gray and I. R. Triay eds. “Scientific Basis for Nuclear Waste Management XX.” Materials Research Society, Pittsburgh, 341-348 (1997b).
12. Xu, H., and Wang, Y., Journal of Nuclear Materials, 275 (1999), 216.
13. Wang, Y., and Xu, H., Thermodynamic stability of actinide pyrochlore minerals in deep geologic repository environments. In D. Shoesmith ed. “Scientific Basis for Nuclear Waste Management XXIII.” Materials Research Society, Pittsburgh, (in press) (1999).
14. Lumpkin, G. R., Smith, K. L., Mark, G., and Blackford, M. G., In T. Murakami and R. C. Ewing eds. “Scientific Basis for Nuclear Waste Management XVIII.” Materials Research Society, Pittsburgh, 885-862 (1995).
15. Solomah, A. G., Sridhar, T. S., and Jones, S. C., In “Advances in Ceramics, vol. 20, Nuclear Waste Management II, American Ceramic Society, Columbus, p. 259 (1996).
16. Hench, L. L., Clarke, D. E., and Campbell, J., Chemical Waste Management, 5 (1984), 149.
17. Xu, H., and Wang, Y., Journal of Nuclear Materials, 279 (2000), 100-106.
18. Fortmer, J. A., Buck, E. C., Ellison, A. J. G., and Bates, J. K., Ultramicroscopy, 67 (1997), 77.
19. Xu, H., Wang, Y., and Barton, L. L., Journal of Nuclear Materials, 265 (1999), 117.
20. Buck, E. C., Chamberlain, D. B., and Giré, R., In D. J. Wronkiewicz and J. H. Lee eds. “Scientific Basis for Nuclear Waste Management XXII.” Materials Research Society, Pittsburgh, 19 (1999).
21. White, T. J., American Mineralogist, 69 (1984), 1156.
22. Bayliss P., Mazzi F., Munno R., White T. J., Mineralogical Magazine , 53 (1989), 565.
23. Xu, H., Wang, Y., and Barton, L. L., Journal of Nuclear Materials, 273 (1999), 343.
24. Knauss K. G., Bourcier W. L., McKeegan K. D., Merzbacher C. I., Nguyen S. N., Ryerson F. J., Smith D. K., Weed H. C., and Newton L. (1990) *Mat. Res. Soc. Symp. Proc.* **176**:371-381.
25. Roberts, S. K., Bourcier, W. L., and Shaw, H. F., Radiochim. Acta., 88 (2000), 539-543.